

# Magnetically Recoverable Fe<sub>3</sub>O<sub>4</sub>-Modified Bentonite as a Heterogeneous Catalyst of H<sub>2</sub>O<sub>2</sub> Activation for Efficient Degradation of Methyl Orange

Linhu Yuan\*

Department of City Construction, Taiyuan City Vocational College,  
Taiyuan 030027, Shanxi, PR China

Received: 22 November 2016

Accepted: 28 March 2017

## Abstract

Clay-based materials provide an efficient and environmentally benign strategy for heterogeneous catalytic oxidation. In this study, a novel Fe<sub>3</sub>O<sub>4</sub>-modified bentonite (Fe<sub>3</sub>O<sub>4</sub>-BT) catalyst was obtained by using the hydrothermal method. The catalyst was characterized by transmission electron microscopy, X-ray diffraction, and Fourier transform infrared spectroscopy. The Fe<sub>3</sub>O<sub>4</sub> nanoparticles mainly existed on the surface and in the outermost pores of the BT, thus exhibiting improved dispersion and lower levels of aggregation. The catalytic activity of Fe<sub>3</sub>O<sub>4</sub>-BT was assessed in the degradation of methyl orange (MO) in the presence of H<sub>2</sub>O<sub>2</sub>. Fe<sub>3</sub>O<sub>4</sub>-BT showed higher MO degradation efficiency than both bare Fe<sub>3</sub>O<sub>4</sub> and BT. The initial H<sub>2</sub>O<sub>2</sub> concentration, catalyst loading, temperature, and initial pH were optimized for the degradation of MO. The MO decolorization rate was still ~90% after the Fe<sub>3</sub>O<sub>4</sub>-BT was reused five times. Additionally, the degree of ferric ion dissolution was only  $3.23 \times 10^{-3}$  mg/L after 60 min. This novel catalyst was easily reclaimed by simple magnetic separation and exhibited good reusability and stability.

**Keywords:** Fe<sub>3</sub>O<sub>4</sub>-bentonite/H<sub>2</sub>O<sub>2</sub>, magnetic, heterogeneous Fenton catalysts, methyl orange, decolorization ratio

## Introduction

The dyeing and printing industries result in the discharge of huge amounts of dyestuff pollutants into water bodies. The removal of these pollutants is both difficult and important because of their intense color, potential mutagenicity, and resistance to biochemical degradation

[1]. Various treatment strategies such as adsorption, coagulation, oxidation, and electrochemical methods have been used for the remediation of dye wastewater [2-4]. Of these, advanced oxidation processes (AOPs) are powerful and attractive techniques for the treatment of high-organic-loading and non-biodegradable wastewater [5-6]. Fenton's reagent is commonly employed in AOP methodology as it degrades nearly all organic compounds owing to its ability to form highly reactive free radicals [7-8]. However, there are several limitations to its application. For example,

\*e-mail: ylh-0011@163.com

its production is cost-intensive and causes secondary pollution [9].

Recently, low-cost minerals or inorganic materials with high degradation efficiencies have attracted increasing interest. As natural microporous substrates, bentonites (BTs) show interesting properties in adsorption and catalysis because of their low-charge-density surfaces [10]. Furthermore, their weak forces and charge deficits can lead to inorganic cations such as  $\text{Na}^+$  and  $\text{Ca}^{2+}$  ions penetrating into their layers to balance the negative charge [4]. Magnetite ( $\text{Fe}_3\text{O}_4$ ) nanoparticles have also attracted increasing attention because  $\text{Fe}_3\text{O}_4$  contains both  $\text{Fe}^{2+}$  and  $\text{Fe}^{3+}$  ions, which are crucial cations for initiation of the Fenton reaction according to the classical Haber-Weiss mechanism [11]. Moreover, when in the inverse spinel crystal structure form, the electrons can transfer between  $\text{Fe}^{2+}$  and  $\text{Fe}^{3+}$  in the octahedral sites, allowing the Fe species to be reversibly oxidized and reduced while maintaining the same structure [12-13]. Additionally,  $\text{Fe}_3\text{O}_4$  nanoparticles are magnetic and can be easily separated from spent reaction solutions by magnetic separation. Thus, combining BT with  $\text{Fe}_3\text{O}_4$  as a catalyst for Fenton-like reactions is a promising strategy for the decontamination of wastewater [14].

In this work,  $\text{Fe}_3\text{O}_4/\text{BT}$  was synthesized by a hydrothermal method and characterized by powder X-ray diffraction (XRD), transmission electron microscopy (TEM), and Fourier transform infrared spectroscopy (FTIR). The catalytic properties of the obtained heterogeneous catalysts were assessed in the peroxide oxidation of methyl orange (MO). The effects of catalyst loading, initial pH, reaction temperature, and oxidant concentration were assessed. Furthermore, the stability and reusability of the catalysts, as well as the degradation mechanism, were also investigated.

## Experimental Procedures

### Materials and Chemicals

BT was purchased from Heishan Wancheng Bentonite Co., Ltd., Liaoning, China. The BT sample was ground and passed through a 120-mesh sieve prior to use. Its cation-exchange capacity (CEC) was 108.4 mmol/100 g BT.  $\text{FeCl}_3 \cdot 6\text{H}_2\text{O}$ , NaOAc, ethylene glycol (EG), polyethylene glycol 200 (PEG200), and epichlorohydrin (ECH) were analytical grade reagents obtained from Tianjin Kernel Chemical reagent Co., Ltd. (Tianjin, China). All the chemicals used in this study were analytical reagent grade and were used without further purification.

The  $\text{Fe}_3\text{O}_4/\text{BT}$  nanocomposite was synthesized by hydrothermal reaction of  $\text{FeCl}_3 \cdot 6\text{H}_2\text{O}$  in the presence of BT. In a typical process, a mixture of 2.16 g  $\text{FeCl}_3 \cdot 6\text{H}_2\text{O}$ , 5.76 g NaOAc, and 1.6 g PEG 200 in 60 mL EG was stirred for 30 min. Then, 0.5 g BT and 1 mL ECH were added to the homogeneous solution and the mixture was stirred at 55°C for 2 h. The mixture was then transferred to a 100 mL autoclave and heated to 200°C for 12 h before

cooling to room temperature, whereupon a dark black solution formed that was then filtered. The precipitate was washed with distilled water/ethanol (1:1) and dried under vacuum at 80°C to obtain the  $\text{Fe}_3\text{O}_4/\text{BT}$  nanocomposite.

### Characterizations and Measurements

The FTIR spectra were recorded between 400 and 4,000  $\text{cm}^{-1}$  from KBr pellets using a Tensor 27 spectrometer (Bruker, Germany). XRD patterns were obtained using a Rigaku Max 2550VB+/PC instrument (Japan) at a scan speed of 8°/min in a  $2\theta$  range of 5-80°. TEM was performed with a JEM-2100 high-resolution transmission electron microscope (JEOL, Japan) at 300 kV.

### Batch Experiments

Batch heterogeneous Fenton experiments for the removal of MO as a model wastewater pollutant were carried out in a 250 mL glass flask reactor (75 mL actual reaction volume) under continuous magnetic mechanical stirring. Typically, an appropriate amount of catalyst suspended in water (0.5 g/L) was placed into the glass reactor. The system was then heated to the appropriate temperature and MO (100 mg/L) and hydrogen peroxide (5.66 g/L) were added to the reactor. Solution samples (1.0 mL) were taken at regular time intervals and, following solid removal, quenched by adding 0.5 mL methanol. The time-dependent concentration of the organic pollutants in the supernatant was analyzed using a UV-Vis spectrophotometer. MO mineralization was followed by measuring the total organic carbon (TOC) with a Shimadzu TOC-5000A analyzer. The TOC results presented are the average of at least three measurements with an accuracy of  $\pm 5\%$ .

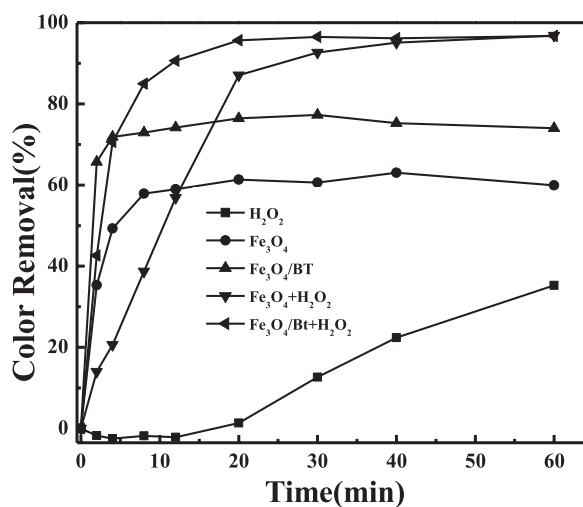


Fig. 1. MO degradation with various catalysts. Reaction conditions: MO = 100 mg/L,  $\text{H}_2\text{O}_2$  = 5.66 g/L, catalyst = 0.50 g/L, T = 25°C, pH = 3.

## Results and Discussion

### Catalyst Evaluation

H<sub>2</sub>O<sub>2</sub>, Fe<sub>3</sub>O<sub>4</sub>, Fe<sub>3</sub>O<sub>4</sub>-BT, Fe<sub>3</sub>O<sub>4</sub>/H<sub>2</sub>O<sub>2</sub>, and Fe<sub>3</sub>O<sub>4</sub>-BT/H<sub>2</sub>O<sub>2</sub> were assessed for the degradation of MO, and the results are shown in Fig. 1. The decolorization rates of MO in the presence of H<sub>2</sub>O<sub>2</sub>, Fe<sub>3</sub>O<sub>4</sub>, Fe<sub>3</sub>O<sub>4</sub>-BT, Fe<sub>3</sub>O<sub>4</sub>/H<sub>2</sub>O<sub>2</sub>, and Fe<sub>3</sub>O<sub>4</sub>-BT/H<sub>2</sub>O<sub>2</sub> are 35.26, 59.93, 74.02, 96.72, and 96.72%, respectively. Fe<sub>3</sub>O<sub>4</sub>-doped BT rapidly destroys the chromophore structure of the dye. A possible reason for this is that Fe<sub>3</sub>O<sub>4</sub> provides Fe for the catalytic reaction and BT enhances MO adsorption [4]. Furthermore, the degradation of MO over Fe<sub>3</sub>O<sub>4</sub>-BT/H<sub>2</sub>O<sub>2</sub> is complete after 20 min, while Fe<sub>3</sub>O<sub>4</sub>/H<sub>2</sub>O<sub>2</sub> needs 40 min. Other samples only slightly improve MO degradation. Thus, Fe<sub>3</sub>O<sub>4</sub>-modified BT exhibits the highest activity. In order to study the effects of the Fe<sub>3</sub>O<sub>4</sub> species on the BT, the samples were analyzed with XRD, FTIR, and TEM.

### Catalyst Characterization

The XRD patterns for Fe<sub>3</sub>O<sub>4</sub>, BT, and Fe<sub>3</sub>O<sub>4</sub>-BT are shown in Fig. 2. BT is mainly composed of montmorillonite (JCPDS file no. 29-1498) and silicon dioxide (JCPDS file No. 46-1045). An interlamellar spacing of 1.16 nm was calculated using Scherer's equation for the (001) diffraction line (6.03°), indicating that the BT is of the Na-based type. The reflections for Fe<sub>3</sub>O<sub>4</sub> can be indexed as cubic phase Fe<sub>3</sub>O<sub>4</sub> (JCPDS file No.19-0629). In the XRD pattern for the Fe<sub>3</sub>O<sub>4</sub>-BT nanocomposite, the reflections corresponding to BT are present at 2θ = 6.03, 19.80, 28.50, and 35.22° [4], and the reflections at 19.80, 28.50, and 35.22° are of lower intensity than those in the pure BT. Peaks for Fe<sub>3</sub>O<sub>4</sub> at 2θ = 34.98, 36.06, 43.25, 57.31, and 61.98° are clearly observed [15-16], indicating that Fe<sub>3</sub>O<sub>4</sub> particles are mainly dispersed on the external surfaces of the BT. Additionally, loading Fe<sub>3</sub>O<sub>4</sub> onto the BT changes its d<sub>001</sub> value from 1.47 to 1.16 nm, indicating that Mg<sup>2+</sup> and Ca<sup>2+</sup> metal ions are replaced by Fe ions that intercalate into the silicate layers. This material structure

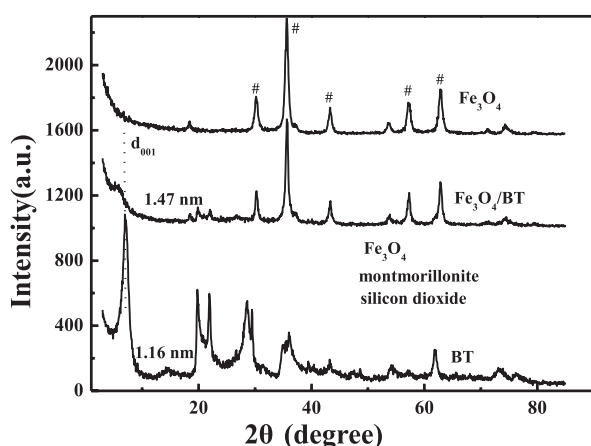


Fig. 2. XRD patterns of BT, Fe<sub>3</sub>O<sub>4</sub>, and Fe<sub>3</sub>O<sub>4</sub>-BT.

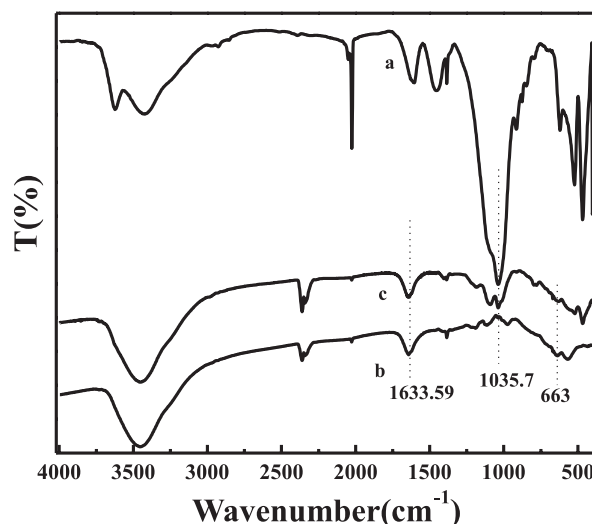


Fig. 3. FTIR spectra of a) BT, b) Fe<sub>3</sub>O<sub>4</sub>, and c) Fe<sub>3</sub>O<sub>4</sub>-BT.

provides more •OH radicals after the introduction of H<sub>2</sub>O<sub>2</sub> because of their more effective contact with Fe<sub>3</sub>O<sub>4</sub>, enhancing catalytic efficiency. Furthermore, the material also maintains its good magnetic responsiveness and recyclability.

FTIR spectroscopy was employed to further confirm the structure of the nanocomposites (Fig. 3). The absorption bands at 3,417.63, 3,450.41, and 1,633.59 cm<sup>-1</sup> can be ascribed to vibrations of water molecules. The absorption bands at 1,035.7 and 791 cm<sup>-1</sup> are Si-O stretching vibrations. The characteristic bands at 576.68 and 663 cm<sup>-1</sup> are due to Fe-O stretching vibrations. The intensities of the Si-O bands in the Fe<sub>3</sub>O<sub>4</sub>-BT nanocomposite are weaker than those of BT, indicating that the Fe-O bonds interact with the Si-O bonds on the surface of the BT [17]. Thus, Fe<sub>3</sub>O<sub>4</sub> is probably bonded to the surface of the BT during the synthesis procedure.

The morphology of the prepared samples was also studied using TEM. Fig. 4b) shows the presence of hollow, spherical, monodispersed Fe<sub>3</sub>O<sub>4</sub> particles with a uniform size of ~200 nm, allowing for improved adsorption of MO. However, as seen from the image of Fe<sub>3</sub>O<sub>4</sub>-BT (Fig. 4c), the spheres tend to be non-uniform and the particles become smaller upon the addition of BT. TEM micrographs of the Fe<sub>3</sub>O<sub>4</sub>-BT composite show that Fe<sub>3</sub>O<sub>4</sub> is uniformly dispersed on the BT surface. These results are in good agreement with the XRD observations.

### Catalytic Behavior

Decreasing the initial pH leads to a much higher degradation rate. A high MO removal efficiency is achieved at pH 3 (Fig. 5). This can be explained by the increased production of oxidizing species at higher pH. However, excessive acidity can cause equipment corrosion, so an optimum pH of 3 was employed.

The effect of H<sub>2</sub>O<sub>2</sub> was analyzed by varying its initial concentration between 1.42 and 11.33 g/L (Fig. 6). The

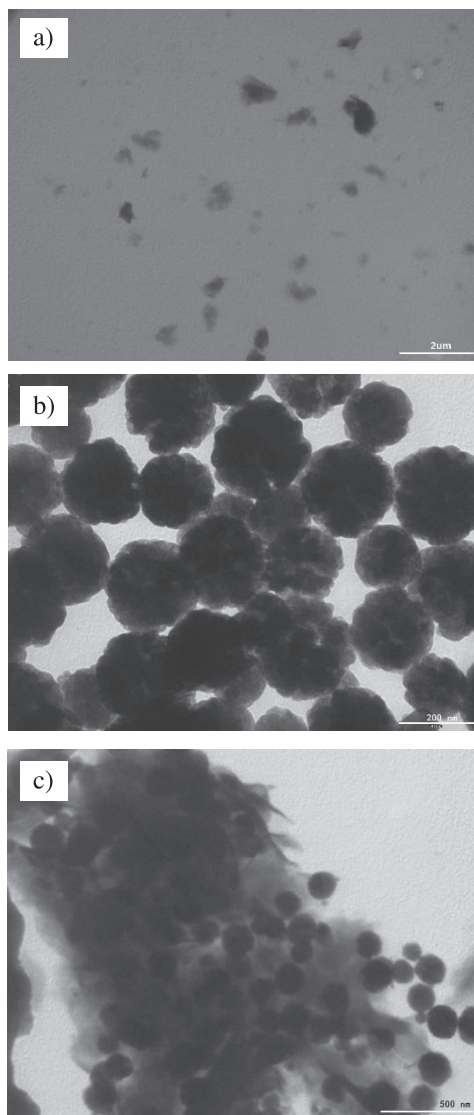


Fig. 4. TEM images of a) BT, b)  $\text{Fe}_3\text{O}_4$ , and c)  $\text{Fe}_3\text{O}_4$ -BT.

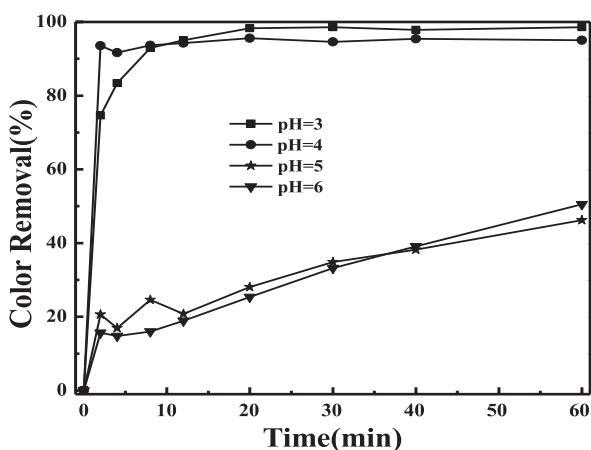


Fig. 5. Effect of initial pH for MO degradation over  $\text{Fe}_3\text{O}_4$ -BT/ $\text{H}_2\text{O}_2$ . Reaction conditions: MO = 100 mg/L,  $\text{H}_2\text{O}_2$  = 11.33 g/L, catalyst = 1.0 g/L, T = 45°C.

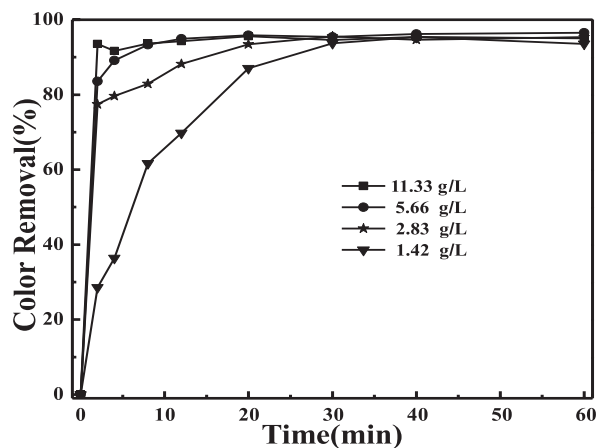


Fig. 6. Influence of  $\text{H}_2\text{O}_2$  content on MO removal. Reaction conditions: MO = 100 mg/L, catalyst = 1.0 g/L, T = 45°C, pH = 3.

MO degradation rate increases significantly when the  $\text{H}_2\text{O}_2$  concentration increases from 1.42 to 11.33 g/L. Clearly, the degradation process is accelerated when the  $\text{H}_2\text{O}_2$  concentration increases to 5.66 g/L. However, the rate constant is slightly reduced at a higher  $\text{H}_2\text{O}_2$  concentration (11.33 g/L). A possible reason for this phenomenon is that the increased  $\text{H}_2\text{O}_2$  concentration induces homogeneous catalytic oxidation. Since MO degradation is directly related to the concentration of the  $\cdot\text{OH}$  produced by the catalytic decomposition of  $\text{H}_2\text{O}_2$ , increased MO decomposition is expected at higher  $\text{H}_2\text{O}_2$  concentration. However, no further improvement occurs when the  $\text{H}_2\text{O}_2$  concentration increases to 11.33 g/L, which can be explained by the scavenging of  $\cdot\text{OH}$  by  $\text{H}_2\text{O}_2$  [18-19]:



The oxidation potential of  $\cdot\text{OOH}$  is much lower than that of  $\cdot\text{OH}$ . Therefore, this slows the reaction. Thus, 5.66 g/L of  $\text{H}_2\text{O}_2$  was deemed optimal in this study.

As expected, the MO degradation rate increases dramatically as the amount of catalyst employed increases from 0.25 to 1.5 g/L (Fig. 7) owing to the increased number of active sites for the formation of  $\cdot\text{OH}$  and, perhaps equally importantly, for MO adsorption and the supply of Fe ions. However, when the catalyst addition is further increased to 1.5 g/L, the degradation of MO does not improve but slightly decreases. This may be due to the agglomeration of nanoparticles and the scavenging of hydroxyl radicals or other radicals by Fe species through the undesirable reactions (2) and (3) [20-21]:



The degradation of MO by  $\text{Fe}_3\text{O}_4$ -BT is dramatically improved with increasing reaction temperature, as seen

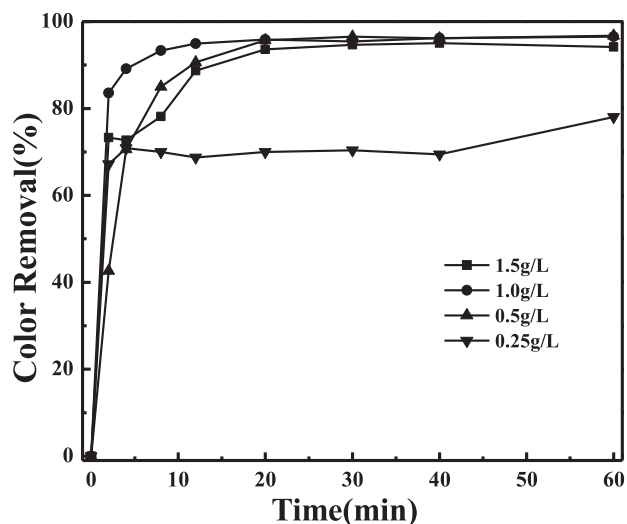


Fig. 7. Influence of  $Fe_3O_4$ -BT content on MO removal. Reaction conditions: MO = 100 mg/L,  $H_2O_2$  = 5.66 g/L, T = 45°C, pH = 3.

from Fig. 8. According to a previous study [4], the change in enthalpy upon the oxidative degradation of MO is positive while the process is endothermic. Accordingly, an increase in reaction temperature is beneficial for the degradation of MO. The optimum temperature is 45°C.

During the decolorization of MO, reaction intermediates that may be long-lived and even more toxic than the parent compound can form. TOC values are similar for BT/ $H_2O_2$ ,  $Fe_3O_4/H_2O_2$ , and  $Fe_3O_4$ -BT (Fig. 9) and slightly lower than those shown for the corresponding heterogeneous Fenton systems. However, a much higher value (~75%) is obtained with the introduction of  $H_2O_2$  to  $Fe_3O_4$ -BT. The highest MO degradation (~97%) is also obtained with this system, although not all degraded MO is mineralized. These interesting results indicate that  $Fe_3O_4$ -BT is a good catalyst for MO removal by homogeneous Fenton

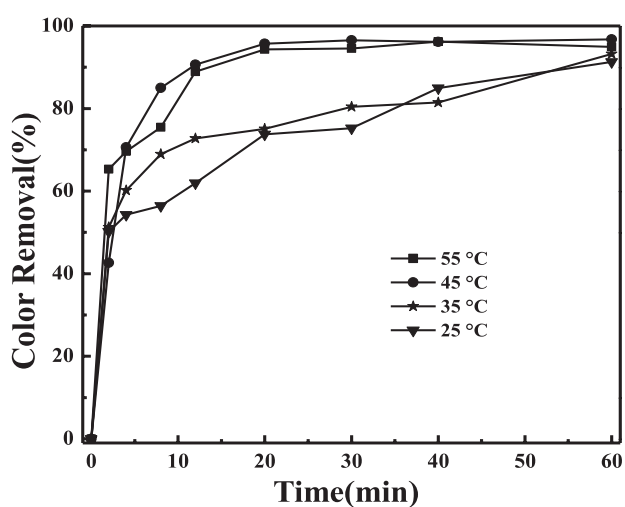


Fig. 8. Influence of reaction temperature on MO removal. Reaction conditions: MO = 100 mg/L,  $H_2O_2$  = 5.66 g/L, catalyst = 0.5 g/L, pH = 3.

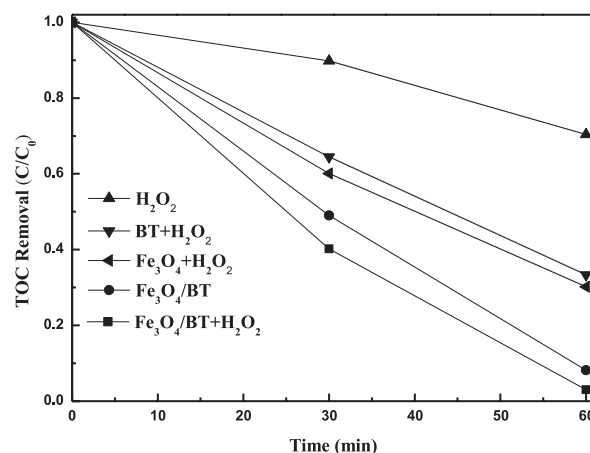


Fig. 9. TOC removal with various catalysts. Reaction conditions: MO = 100 mg/L,  $H_2O_2$  = 5.66 g/L, catalyst = 0.50 g/L, T = 45°C, pH = 3.

oxidation. This catalyst causes  $H_2O_2$  to generate many hydroxyl radicals, and may therefore exhibit a synergic effect of  $H_2O_2$  oxidation and  $Fe_3O_4$ -BT adsorption, which is favorable for attacking aromatic compounds and thus improving MO degradation.

#### Reusability of Catalyst

The reusability of a heterogeneous catalyst is crucial for its practical application. To evaluate the catalytic stability of the  $Fe_3O_4$ -BT catalyst in the  $H_2O_2$  oxidation system, the particles were repeatedly recovered to perform successive MO degradation tests. The obtained results are shown in Fig. 11. An MO decolorization efficiency of 89.94% is achieved after the fifth run.

Additionally, it is believed that the ferric content of a catalyst can undergo microphase separation, leading to deactivation. Consequently, it is necessary to evaluate the ferric content after the reaction. The ferric content of  $Fe_3O_4$ -

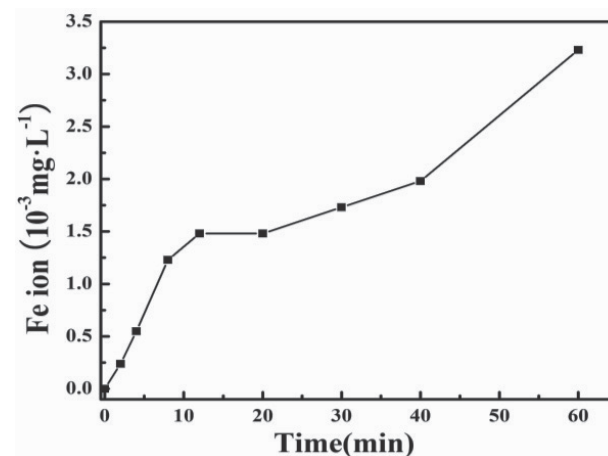


Fig. 10. Amount of dissolved Ferric ion in solution. Reaction conditions: MO = 100 mg/L,  $H_2O_2$  = 5.66 g/L, catalyst = 0.50 g/L, T = 45°C, pH = 3.

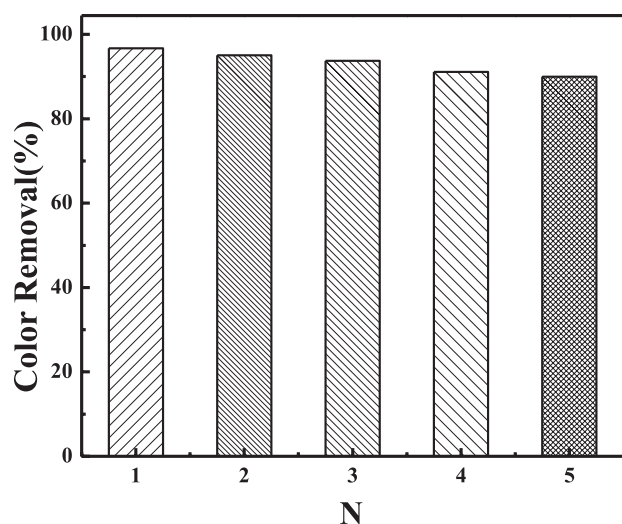
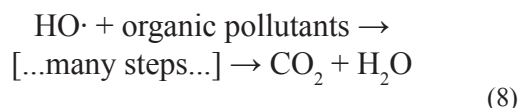
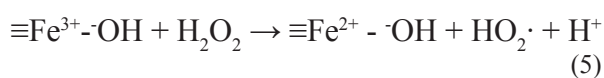
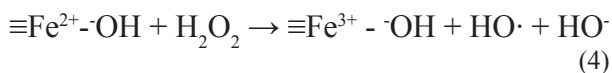


Fig. 11. Reuse of Fe<sub>3</sub>O<sub>4</sub>-BT. Reaction conditions: MO = 100 mg/L, H<sub>2</sub>O<sub>2</sub> = 5.66 g/L, catalyst = 0.50 g/L, T = 45°C, pH = 3.

BT was measured before and after the catalytic reaction using inductively coupled plasma elemental analysis. The ferric ion dissolution is only  $3.23 \times 10^{-3}$  mg/L after a 60 min reaction (Fig. 10.), indicating that Fe<sub>3</sub>O<sub>4</sub>-BT has good chemical stability and reusability.

### Reaction Mechanism

Many previous studies [22-25] have shown that the primary HO• radical plays a significant role in the oxidation of organic compounds. Catalytic H<sub>2</sub>O<sub>2</sub> activation through the reduction of Fe<sup>3+</sup> to Fe<sup>2+</sup> is thermodynamically favorable. The binding of ≡Fe<sup>2+</sup> to surface hydroxyl groups (OH) through the dissociative adsorption of water molecules on the Fe<sub>3</sub>O<sub>4</sub>-BT surface is expected to change with the oxidation state of the surface metal [26-27]. The ≡Fe<sup>2+</sup> species on the Fe<sub>3</sub>O<sub>4</sub>-BT surface react with H<sub>2</sub>O<sub>2</sub> to produce surface-bound HO•, and some more ≡Fe<sup>3+</sup> species can be produced from the formed ≡Fe<sup>2+</sup> species upon reaction with H<sub>2</sub>O<sub>2</sub> (Eq. (4)). ≡Fe<sup>3+</sup> is then reduced back to ≡Fe<sup>2+</sup> by another molecule of H<sub>2</sub>O<sub>2</sub>, forming a hydroperoxyl radical and a proton (Eq. (5)). But the reactions represented by Eq. (6) and Eq. (7) efficiently consume hydroxyl radicals. Therefore, in practical applications of the Fenton reaction, catalytic amounts of iron salts are typically used and H<sub>2</sub>O<sub>2</sub> is added slowly to the system. This is one of the reasons that Fe<sub>3</sub>O<sub>4</sub>-BT exhibits good stability and recyclability.



### Conclusions

A novel heterogeneous Fenton catalyst (Fe<sub>3</sub>O<sub>4</sub>-BT) has been synthesized via a hydrothermal method and characterized by XRD, FTIR, and TEM. The results show that the Fe<sub>3</sub>O<sub>4</sub> pillaring process leads to an increase of the *d*<sub>001</sub> spacing. Furthermore, the pure Fe<sub>3</sub>O<sub>4</sub> synthesized is distributed uniformly on the surface of the BT. The optimum reaction conditions for the degradation of MO were found to be an initial pH of 3, Fe<sub>3</sub>O<sub>4</sub>-BT dosage of 0.5 g/L, an initial H<sub>2</sub>O<sub>2</sub> concentration of 5.66 g/L, an initial methyl orange concentration of 100 mg/L, and a reaction temperature of 45°C. The Fe<sub>3</sub>O<sub>4</sub>-BT was reused five times by magnetic separation, and maintained an MO decolorization rate of 89.94%. Additionally, the quantity of ferric ion dissolution was only  $3.23 \times 10^{-3}$  mg/L after 60 min, which is insignificant in comparison to the amount of Fe<sub>3</sub>O<sub>4</sub>/BT added. The results confirm that Fe<sub>3</sub>O<sub>4</sub>-BT exhibits good catalytic activity and stability.

### References

1. AI L.H., ZHANG C.Y., CHEN Z.L. Removal of Methylene Blue from aqueous solution by a solvothermal-synthesized graphene/magnetite Composite. *J. Hazard. Mater.* **192** (3), 1515, **2011**.
2. AI L.H., ZHOU C.Y., JIANG J. Removal of Methylene Blue from aqueous solution by montmorillonite/CoFe<sub>2</sub>O<sub>4</sub> composite with magnetic separation performance. *Desalination*. **266** (1-3), 72, **2011**.
3. BRILLAS E., SIRÉS I., OTURAN M.A. Electro-Fenton process and related electrochemical technologies based on Fenton's reaction chemistry. *Desalination*. **109** (12), 6570, **2009**.
4. CHANG J.L., MA J.C., MA Q.L., ZHANG D.D., QIAO N.N., HU M.X., MA H.Z. Adsorption of Methylene Blue onto Fe<sub>3</sub>O<sub>4</sub>/activated montmorillonite nanocomposite. *Appl. Clay. Sci.* **119** (1), 132, **2016**.
5. WANG Y.J., ZHAO H.Y., GAO J.X., ZHAO G.H., ZHANG Y.G., ZHANG Y.L. Rapid mineralization of azo-dye wastewater by microwave synergistic electro-Fenton oxidation process. *J. Phys. Chem. C*. **116** (13), 7457, **2012**.
6. TUŠAR N.N., MAUC'EC D., RANGUS M., ARC'ON I., MAZAJ M., COTMAN M., PINTAR A., KAUC'IC V. Manganese functionalized silicate nanoparticles as a Fenton-type catalyst for water purification by advanced oxidation processes (AOP). *Adv. Funct. Mater.* **22** (4), 820, **2012**.
7. ZHANG T., ZHU H., CROUÉ J.-P. Production of sulfate radical from peroxymonosulfate induced by a magnetically separable CuFe<sub>2</sub>O<sub>4</sub> spinel in water: Efficiency, stability, and mechanism. *Environ. Sci. Technol.* **47** (6), 2784, **2013**.
8. YAO Y.J., CAI Y.M., WEI F.Y., WEI F.Y., WANG X.Y., WANG S.B. Magnetic recoverable MnFe<sub>2</sub>O<sub>4</sub> and MnFe<sub>2</sub>O<sub>4</sub>-graphene hybrid as heterogeneous catalysts of

- peroxymonosulfate activation for efficient degradation of aqueous organic pollutants. *J. Hazard. Mater.* **270**, 61, **2014**.
9. YUAN S.H., FAN Y., ZHANG Y.C., MAN T., PENG L. Pd-Catalytic *in situ* generation of H<sub>2</sub>O<sub>2</sub> from H<sub>2</sub> and O<sub>2</sub> produced by water electrolysis for the efficient electro-Fenton degradation of Rhodamine B. *Environ. Sci. Technol.* **45** (19), 8514, **2011**.
  10. GLADYSZ-PLASKA A., OSZCZAK A., FUKS L., MAJDAN M. New effective sorbents for removal of Am-241 from drinking water. *Pol. J. Environ. Stud.* **25** (6), 2401, 2016.
  11. LEE S.M., TIWARI D. Organo and inorgano-organo-modified clays in the remediation of aqueous solutions: An overview. *Appl. Clay Sci.* **59–60**, 84, **2012**.
  12. LI W.B., WAN D., WANG G.H., CHEN K., HU Q.M., LU L.L. Heterogeneous Fenton degradation of Orange II by immobilization of Fe<sub>3</sub>O<sub>4</sub> nanoparticles onto Al-Fe pillared bentonite. *Korean J. Chem. Eng.* **33** (5), 1557, **2016**.
  13. ZHANG J.B., ZHUANG J., GAO L., ZHANG Y., GU N., FENG J., YANG D.L., ZHU J.D., YAN X.Y. Decomposing phenol by the hidden talent of ferromagnetic nanoparticles original. *Chemosphere.* **73** (9), 1524, **2008**.
  14. WU W., WU Z.H., YU T.Y., JIANG C.Z., KIM W-S. Recent progress on magnetic iron oxide nanoparticles: Synthesis, surface functional strategies and biomedical applications. *Sci. Technol. Adv. Mater.* **16** (2), 1, **2015**.
  15. KAUR R., HASAN A., IQBAL N., IQBAL N., ALAM S., SAINI M.K., RAZA S.K. Synthesis and surface engineering of magnetic nanoparticles for environmental cleanup and pesticide residue analysis: A review. *J. Sep. Sci.* **37** (14), 1805, **2014**.
  16. MA J.C., WANG L.L., WU Y.L., ZHAO X.D., DONG X.S., ZHANG J.L., ZHANG Q.F., QIAO C., MA Q.L. Role of precipitant species on the coprecipitation for preparing Fe<sub>3</sub>O<sub>4</sub> nanoparticles. *Optoelectron. Adv. Mat.* **8** (11-12), 1077, **2014**.
  17. MA J.C., WANG L.L., WU Y.L., DONG X.S., MA Q.L., QIAO C., ZHANG Q.F., ZHANG J.L. Facile synthesis of Fe<sub>3</sub>O<sub>4</sub> nanoparticles with a high specific surface area. *Mater. Trans.* **55** (12), 1900, **2014**.
  18. XUAN S., HAO L., JIANG W., GONG X.L., HUA Y., CHEN Z.Y. Preparation of water-soluble magnetite nanocrystals through hydrothermal approach. *J. Magn. Magn. Mater.* **308** (2), 210, **2007**.
  19. ELMOLLA E., CHAUDHURI M. Optimization of Fenton process for treatment of amoxicillin, ampicillin and cloxacillin antibiotics in aqueous solution. *J. Hazard. Mater.* **170** (2), 666, **2009**.
  20. HUANG R.X., FANG Z.Q., YAN X.M., CHENG W. Heterogeneous Sono-Fenton catalytic degradation of bisphenol A by Fe<sub>3</sub>O<sub>4</sub> magnetic nanoparticles under neutral condition. *Chem. Eng. J.* **197**, 242, **2012**.
  21. HERMANEK M., ZBORIL R., MEDRIK I., PECHOUSEK J., GREGOR C. Catalytic efficiency of iron(III) oxides in decomposition of hydrogen peroxide: Competition between the surface area and crystallinity of nanoparticles. *J. Am. Chem. Soc.* **129** (35), 10929, **2007**.
  22. SUN S-P., LEMLEY A.T. p-Nitrophenol degradation by a heterogeneous Fenton-like reaction on nano-magnetite: Process optimization, kinetics, and degradation pathways. *J. Mol. Catal. A Chem.* **349** (1), 71, **2011**.
  23. KANG N., LEE D.S., YOON J. Kinetic modeling of Fenton oxidation of phenol and monochlorophenols. *Chemosphere.* **47** (9), 915, **2002**.
  24. LAAT J., LE T.G. Effects of Chloride Ions on the Iron(III)-catalyzed Decomposition of Hydrogen Peroxide and on the Efficiency of the Fenton-like Oxidation Process. *Appl. Catal., B.* **66** (1-2), 137, **2006**.
  25. FRIEDRICH L.C., MENDES M.A., SILVA V.O., Zanta C.L.P.S., Jr A.M., Quina F.H. Mechanistic implications of zinc(II) ions on the degradation of phenol by the Fenton reaction. *J. Braz. Chem. Soc.* **23** (7), 1372, **2012**.
  26. BARBUSIŃSKI K. The modified Fenton process for decolorization of dye wastewater. *Pol. J. Environ. Stud.* **25** (1), 9, **2016**.
  27. AI Z.H., GAO Z.T., ZHANG L.Z., HE W.W., YIN J.J. Core-shell structure dependent reactivity of Fe@Fe<sub>2</sub>O<sub>3</sub> nanowires on aerobic degradation of 4-chlorophenol. *Environ. Sci. Technol.* **47** (10), 5344, **2013**.